

The Influence of a Grinding Notch on the Gear Bending Strength Rating

Ulrich Kissling and Ioannis Zotos

Introduction

To achieve the requested quality, most gears today are ground. The usual grinding process includes treating the gear flank but disengaging before reaching the root rounding area. If the gear is pre-manufactured with a tool without protuberance, then at the position where the grinding tool retracts from the flank a grinding notch in the tooth root area is produced. Such a notch may increase the bending stresses in the root area, thus reducing the strength rating.

The AGMA 2001 standard does not address this topic, but in ISO 6336-3, a rule to consider the stress increase due to a grinding notch is documented. The formulas presented are based on research done by Wirth in the 1970s. A recent discussion in the ISO Workgroup responsible for the development of this standard showed that a review of the formulas is necessary as it is presently, the method can be interpreted in two ways.

Modern FEM (finite element method) tools are well-adapted to calculate the stress in the root area, so it is possible to perform an FEM-based parametric study to compare the grinding notch effect as calculated by FEM with the formulas of the standard. Additionally, in Wirth's work some factors are given that are currently not considered in the standard; this is an additional topic of this investigation.

To make such a study possible, an option for an external FEM software was introduced in a calculation software for strength analysis (ISO 6336). The necessary data, such as the exact tooth form and the load at the highest point of single tooth contact, is transferred to the pre-processor, which automatically generates the mesh and calls the solver and the post-processor. The main results are the stress at the 30° (60° for internal gears) tangent point and the maximum stress found in the overall root area. The

Symbols used in this paper:

Symbol	Description	Unit
Symbols for the grinding notch		
Y_{Sg}	Stress correction factor for gears with grinding notch (ISO 6336)	
Y_S	Stress correction factor for gears without grinding notch (ISO 6336)	
t_g	Grinding notch depth	mm
ρ_g	Grinding notch radius	mm
h_{grind}^*	Height of grinding tool	(in module)
ρ_{grind}^*	Tip radius of grinding tool	(in module)
q	Grinding allowance q	mm
σ_{F0}	Nominal tooth root stress (without load factors K_A, K_V etc.)	
Symbols for gear geometry		
$z, b, m_{nv} \dots$	All symbols according ISO21771 (Ref. 13)	

maximum stress is typically located at the position of the grinding notch.

For helical gears, according to the procedure given in ISO 6336-3, the tooth form of the equivalent spur gear is generated and used for the analysis. An additional topic of interest is the following: if a 3-D FEM analysis is useful for helical gears, how well will the results of the FEM correspond to the equivalent spur gear model used by ISO 6336? This is currently under investigation and will be published later.

In the parameter study for different gear geometries, the grinding allowance, the tip radius of the grinding wheel, the grinding process (generating and form grinding), and the grinding depth were varied. The results provide a good overview of the accuracy of the outcome of the two interpretation variants of the ISO method for the influence of the grinding notch — compared to FEM results. Based on the study, the best variant can be demonstrated. The formula used to obtain the grinding notch depth used in the ISO method is deduced and will be presented. The position of the notch on the tooth has an important influence, which can now be much better considered.

To get a high-torque capacity for today's gears in car transmissions, industrial gearboxes, or wind turbines,

case-carburized steel materials are used. Such gears are pre-manufactured, then case-carburized and surface-hardened. The hardening process generates relatively large distortions of the gears due to the high temperatures during treatment. A gear having quality 7 (AGMA 2015) (Ref. 2) before treatment will typically rise to quality 9 afterwards. To realize a good contact pattern (for high-torque capacity) and low noise behavior, such gears must be reshaped by grinding (or a similar process).

Research on the Grinding Notch Effect

The effect of a grinding notch on the tooth bending load capacity was researched by Wirth (Ref. 1) at the FZG in Munich in the 1970s. Wirth made many measurements on gears with and without grinding notches and deduced S/N-curves. He tested gears with module 3 mm on a test bench, and other gears with module 8 mm were measured on a pulsator. Wirth deduced the stress in the tooth root with the photo-elastic method. Today, the preferred tool to analyze tooth root stress theoretically would be the FE method. But in the 1970s this method was not yet fully accepted, so Wirth used the photo-elastic method to investigate the stress. While the method can be

used to indicate the position of the highest stress, the results obtained with this method are limited.

Wirth's test gears were ground on Maag grinding machines; the Maag dry grinding process was popular at that time but is clearly outdated today. The pre-manufacturing tools used are well-defined, but the shape obtained by the grinding process was documented by contrast pictures only, so the shape, position, and radius of the grinding notch on the different test gears can only be roughly estimated. A profile measurement documentation from an involute measuring machine is not available.

We tried to recalculate Wirth's test gears, but, as the exact tooth form after the grinding process is not defined as precisely as needed, this is unfortunately not possible. Therefore, it is not possible today to recalculate the test gears with an FEM analysis. So, Wirth's impressive research work is of little use today if we try to reproduce his findings with modern calculation methods.

Consideration of the Grinding Notch Effect in ISO 6336-3

In the German DIN 3990-3 (Ref. 3) standard, a rule is included for the consideration of the stress increase due to a grinding notch; the same rule was later included in ISO 6336-3 (Ref. 4). Per the references, the method is based on a work performed by Puchner/Kamenski (Ref. 5), published some years earlier than Wirth's work. Puchner investigated the effect of a notch situated in the center of a bigger notch in general—not on gears. So basically, his results can be applied to the grinding notch case only if the normal to the 30° tangent point in the root rounding and normal to the 30° tangent point of the grinding notch coincide. Wirth (Ref. 1, pp. 6–7) documents the formulas as used 1975 in a working document for the ISO 6336-3 standard. But the formulas that were published in the first official ISO 6336 edition in 1996 are quite different from the equations as documented by Wirth. As a result, some changes were made later, based on the findings of Wirth and others.

The description of the grinding notch effect in ISO 6336-3 is not easily understood, unfortunately, and can be interpreted in various ways. With a grinding

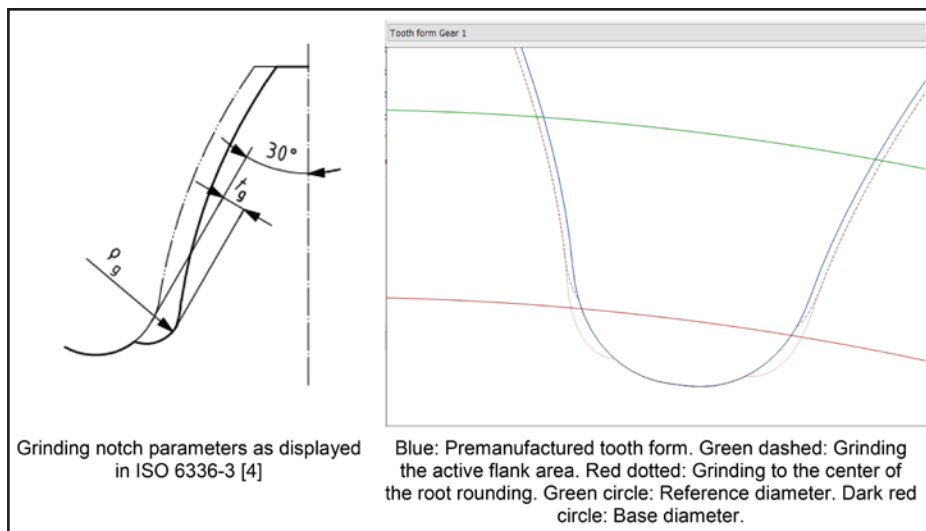


Figure 1 A (left): grinding notch parameters; B (right): different positions of the grinding notch.

notch the stress concentration factor must be substituted by Y_{Sg} , according to Equation 1. The sketch (Fig. 1a) in ISO 6336-3 (Ref. 4) shows the two important parameters used in the grinding notch formula: 1) the maximum depth of grinding notch (t_g); and 2) the radius of grinding notch (ρ_g). The depth t_g is indicated as the distance between the 30° tangent at the pre-manufactured tooth form and the 30° tangent at the grinding notch.

$$Y_{Sg} = \frac{1.3Y_s}{1.3 - 0.6 \sqrt{\frac{t_g}{\rho_g}}} \quad (1)$$

There is no indication on how to calculate t_g and ρ_g in the standard. For a generating grinding process, the radius ρ_g can be calculated, as described in chapter 6 of ISO 6336-3, just using the tooth reference profile deduced from the grinding tool (using $h_{fp} = h_{ap0}$: tip height of the grinding tool; $\rho_{fp} = \rho_{ap0}$: tip radius of the grinding tool). The position of the point where the 30° tangent contacts the tooth (at the critical section) can be deduced with the tooth root chord s_{Fn} , the bending moment arm $h_{F\sigma}$, and the load direction angle $\alpha_{F\sigma n}$. These points must first be calculated for the pre-manufactured tooth and the grinding notch, then the distance between the 30° tangents through these points is the grinding notch depth t_g .

In a recent meeting of the ISO workgroup TC60/WG6, the calculation of the grinding notch effect was discussed. It became evident that two different interpretations were possible. Experts (Interpretation I) from the German gear industry claimed that t_g and ρ_g must be

taken from the printout of the profile measuring machine. In that case, t_g will always approximately correspond to the grinding allowance, and the radius ρ_g , measured on the profile diagram, will be inaccurate because it is slightly changed due to the transformation in the profile measuring machine. The position of the grinding notch, whether higher up on the tooth or not, will then not be considered.

Other experts (Interpretation II) claim that the pre-manufactured tooth and the grinding notch form should be calculated, using t_g as the distance between the tangents described above. The well-known software *STplus* (Ref. 6), developed by FZG in Munich, and the software *KISSsoft* (Ref. 7) are using this method. The approach considers the position of the grinding notch, i.e.—the bigger the distance between notch (higher up) and gear root area, the smaller is t_g ; therefore, the smaller the grinding notch factor becomes.

Both interpretations will yield the same result if the grinding notch is very deep in the root area, in the center of the root rounding (Fig. 1b, dotted line). But standard practice in grinding is to NOT do that; normally, only the active range of the tooth flank is ground. The grinder will emerge out of the flank shortly after the active root diameter (d_{Nf}) is reached (Fig. 1b, dashed line). Figure 1b (dashed line) shows a normal case of a gear having a tip clearance of 0.25^*m_n to the meshing gear. The position of the usual grind notch is at a distance from the root rounding area. It is evident that

Interpretation I is on the safe side, but probably for most practical cases it is *too* conservative.

It is evident that the history of the development of Equation 1 as the interpretation of t_g in Figure 1 is not so clear. We therefore decided to calculate some typical gearsets — using Interpretation I and Interpretation II — and to also compare the results with an FEM approach.

Root Stress Calculation by 2-D Finite Element Method

To minimize the risk of errors by handling a big number of gear calculations in a calculation software according to ISO 6336 and in parallel with an FEM software, we decided to integrate directly an FEM calculation into the *KISSsoft* (Ref. 7) software, i.e. — a gearset is calculated according to ISO 6336, after which the tooth form is generated and then transmitted

to an external FEM program. The FEM program selected is *code aster*, which has a wide user base and can be controlled through scripts (Ref. 10). For the same reasons, the program *Salome* (Ref. 11) was selected for the pre-processing (geometry handling and FE mesh generation).

The accuracy in the generated tooth profile is of great importance for the accurate calculation of stresses in gears, since even the smallest inaccuracies can lead to virtual stress concentration areas — thus influencing the results. For that reason we were based on the advanced tooth form calculation capabilities of *KISSsoft* (Ref. 7). Figure 2 presents the difference in the generated tooth form when using polygon lines vs. cubic splines to export the tooth form.

In the case of polygon lines, the highlighted areas result in stress peaks that do not represent real stresses (Fig. 2, right);

hence it was decided to proceed using cubic splines for the tooth form export.

Regarding the analysis type used, it was decided to proceed in a first step with the 2-D plane stress assumption. That way, the computational time is shorter and more cases can be computed in a shorter time. Beyond that, 2-D plane stress is a common assumption for gear tooth stress analysis (Ref. 12); the smaller the gear face width, the closer to reality is this approximation.

For the FE mesh generation process, an automatic meshing procedure was selected based on the *NETGEN* algorithm. Since there was a need for the mesh generation to work flawlessly for many different cases, it was decided to prefer second-order triangular over quadrangle elements, since it is known that the latter option could result in highly distorted elements in case of abrupt geometry changes (as, for example, in the grinding notch area). The minimum and maximum element sizes were selected based on the normal module of the gear analyzed, whereas a mesh refinement was performed in the stress concentration areas. In order to reduce the size of the generated mesh, only a segment of three teeth of the complete gear is analyzed. That way we manage to reduce the calculation time without losing the information of the area surrounding the root of the loaded tooth. By choice of the user, the gear is clamped either in the inner diameter or at the sides of the segment analyzed (Fig. 3). Also, the mesh density can be selected by the user, i.e. — with ‘very high density’ about 24 nodes are generated in the root rounding area; the total number of elements is 4,000; other choices are ‘high density’ (17 nodes, 2,200 elements) and ‘medium density’ (10 nodes, 1,300 elements).

After the mesh generation is completed, specific nodes are moved to the exact location where results are to be extracted, such as at the 30° tangent point. Since in stress concentration areas (like the grinding notch), there is a high gradient in stresses and the exact location of the extracted result plays an important role (Fig. 4). The mesh refinement at the stress concentration, together with the selection of triangular elements and the performed mesh quality checks, guarantee that this node movement does not affect the accuracy of

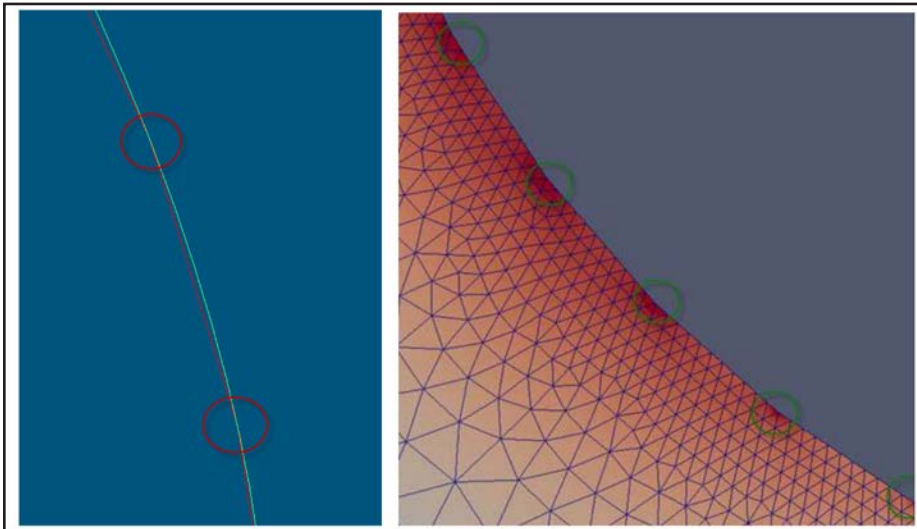


Figure 2 Polygon lines vs. cubic splines in tooth form export.

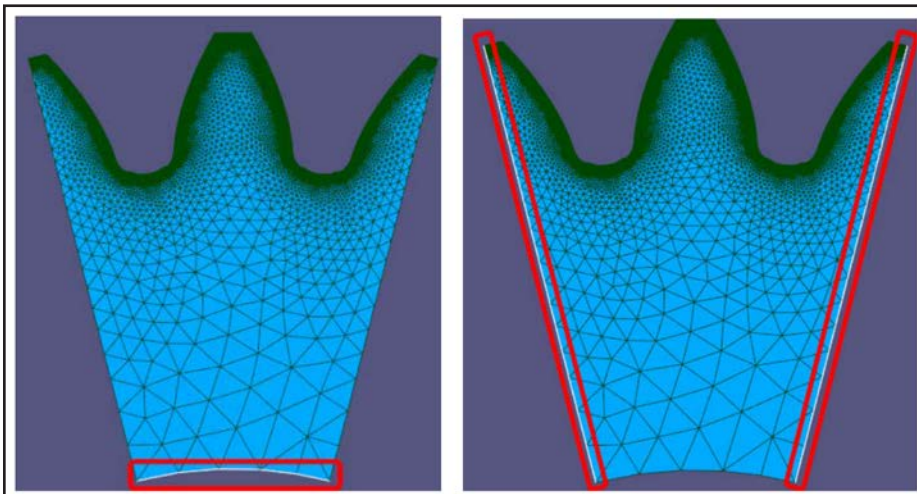


Figure 3 Two different options for clamping locations.

the resulting mesh.

Spur gears. Spur gears are ideal for a 2-D FEM analysis, because the load distribution over the face width is not a topic of this investigation. As in ISO 6336 (Ref. 4), the line load F_n/b ($F_n/b = F_t/\cos(\alpha_n)/b$) is applied at the outer point of single pair tooth contact (HPSTC). The load application angle α_{Fen} according to ISO is used. AGMA 908 (Ref. 8) allows, for spur gears, the choice between load application at tip or at HPSTC. For this investigation only the more accurate method with load application at HPSTC is used. The load angle ϕ_{nL} of AGMA is identical with α_{Fen} of ISO, so the applied load is also F_n/b .

Helical gears. For helical gears, both standards — ISO and AGMA — are converting the helical geometry into a virtual spur gear. The virtual gear is a spur gear having the same tooth form (tooth height and tooth thickness) as the helical tooth in the normal section. Then, to get the stresses, the same formulas are used as for native spur gears.

Therefore, for the FEM analysis we transform the gear geometry into the virtual spur gear (as given by the rules in ISO or AGMA). The tooth form of the virtual gear is then generated and transferred to the FEM procedure. The load, load position at HPSTC, and load angle in the FEM model are transferred, as described for the spur gears.

Calculating the bending stress in the root area, using the virtual spur gears for helical gears, is a certain simplification. That is why both the ISO and AGMA standards use an additional factor to compensate for the difference in stress obtained on the virtual spur gear and the effective stress in a helical gear. In ISO, the stress obtained on the virtual gear is multiplied with helix angle factor Y_β . In AGMA, the stress is multiplied by $1/(C_\psi * K_\psi)$ (C_ψ : helical overlap ratio, K_ψ : helix angle factor (Ref. 8)). Therefore, the stresses obtained by FEM in the documentation are multiplied with these factors to provide values that can be compared to the stresses, as given by ISO or AGMA.

It is clearly interesting to compare stresses obtained by the standard for helical gears with a 3-D/FEM analysis. That is why we decided to have an option in the software to generate data for a 3-D analysis, which is discussed further on.

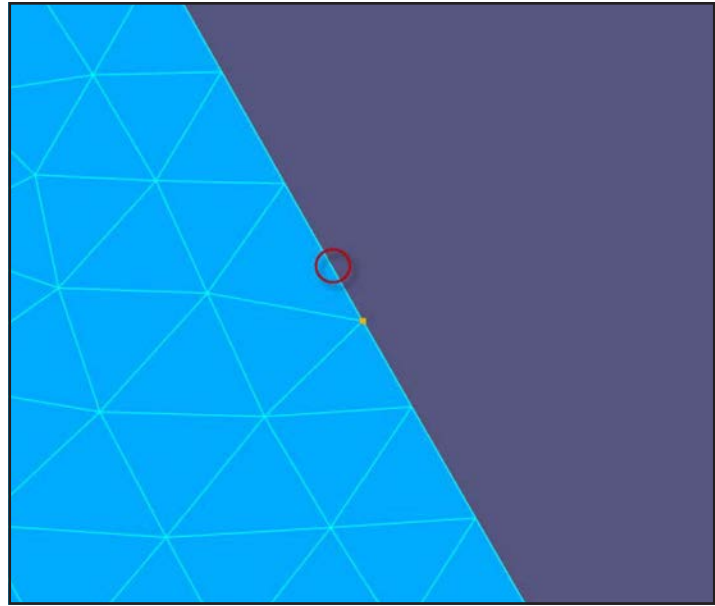


Figure 4 Initial and final location of moved node.

Table 1 Basic gearsets data										
	Module	z_1	x_1	z_2	x_2	h_{aP}^*	h_{fP}^*	ρ_{fP}^*	α_n	β
Set Ia	2 mm	12	0.3	varied	-0.3	1.0	1.25	0.38	20°	0°
Set Ib	2 mm	12	0.3	varied	0.0	1.0	1.25	0.38	20°	0°
Set Ic	2 mm	12	0.3	varied	+0.3	1.0	1.25	0.38	20°	0°
Set Id	2 mm	12	0.3	varied	-0.3	1.0	1.25	0.10	20°	0°
Set Ie	2 mm	12	0.3	varied	0.0	1.0	1.25	0.10	20°	0°
Set If	2 mm	12	0.3	varied	+0.3	1.0	1.25	0.10	20°	0°
	Module	z_1	x_1	z_2	x_2	h_{aP}^*	h_{fP}^*	ρ_{fP}^*	α_n	β
Set 2a	6 mm	25	0.25	varied	0.0	1.0	1.25	0.38	20°	0°
Set 2b	6 mm	25	0.25	varied	0.0	1.0	1.25	0.10	20°	0°
Set 2c	6 mm	25	0.25	varied	0.0	1.0	1.25	0.10	25°	0°
Set 2d	6 mm	25	0.25	varied	0.0	1.0	1.25	0.10	20°	20°

Comparing Gear Stress According to ISO 6336 and AGMA 2101 with 2-D/FEM Results (on Gears without Grinding Notch)

The aim of this investigation is the evaluation of the grinding notch effect. Before performing this task we wanted to test the FEM method used with 'normal' tooth forms and compare the results with ISO 6336 and AGMA 2001. For a good test, we wanted to check a wide range of examples, but this is difficult as FEM calculations are time-consuming.

We therefore decided to integrate the entire calculation procedure in an Excel calculation in order to automatically calculate multiple variants and to control interesting inputs and outputs. This is possible using the COM interface of KISSsoft (Ref. 7). The Excel application permits us to load a gear pair example and then execute through dll-calls an ISO 6336, an AGMA 2001, and finally — a call of the tooth form calculator with appended FEM calculation.

Gear parameters can be changed automatically, step by step; the calculations can be performed and the results can be stored and displayed in an Excel graphic. We selected several basic gearsets (Table 1) and varied, with the Excel application, the tooth number of the gear (from 16 to 200 teeth) in six steps. Thus we obtained results from multiple gearsets and could verify the best possible FEM method.

In the graphics, the following results are displayed on the Y-axis:

- **From FEM:** the maximum stress on the gear found in the root area, the stress at the 30° tangent point according ISO 6336, and the stress at the Lewis parabola point according AGMA908.
- **From ISO 6336:** The nominal tooth root stress σ_{F0} .
- **From AGMA 2001:** The nominal bending stress number σ_{F0} (equal to σ_F , if all K-factors are in unity)

On the X-axis, the tooth number of the gear is displayed.

The results displayed in Figure 5a–5f

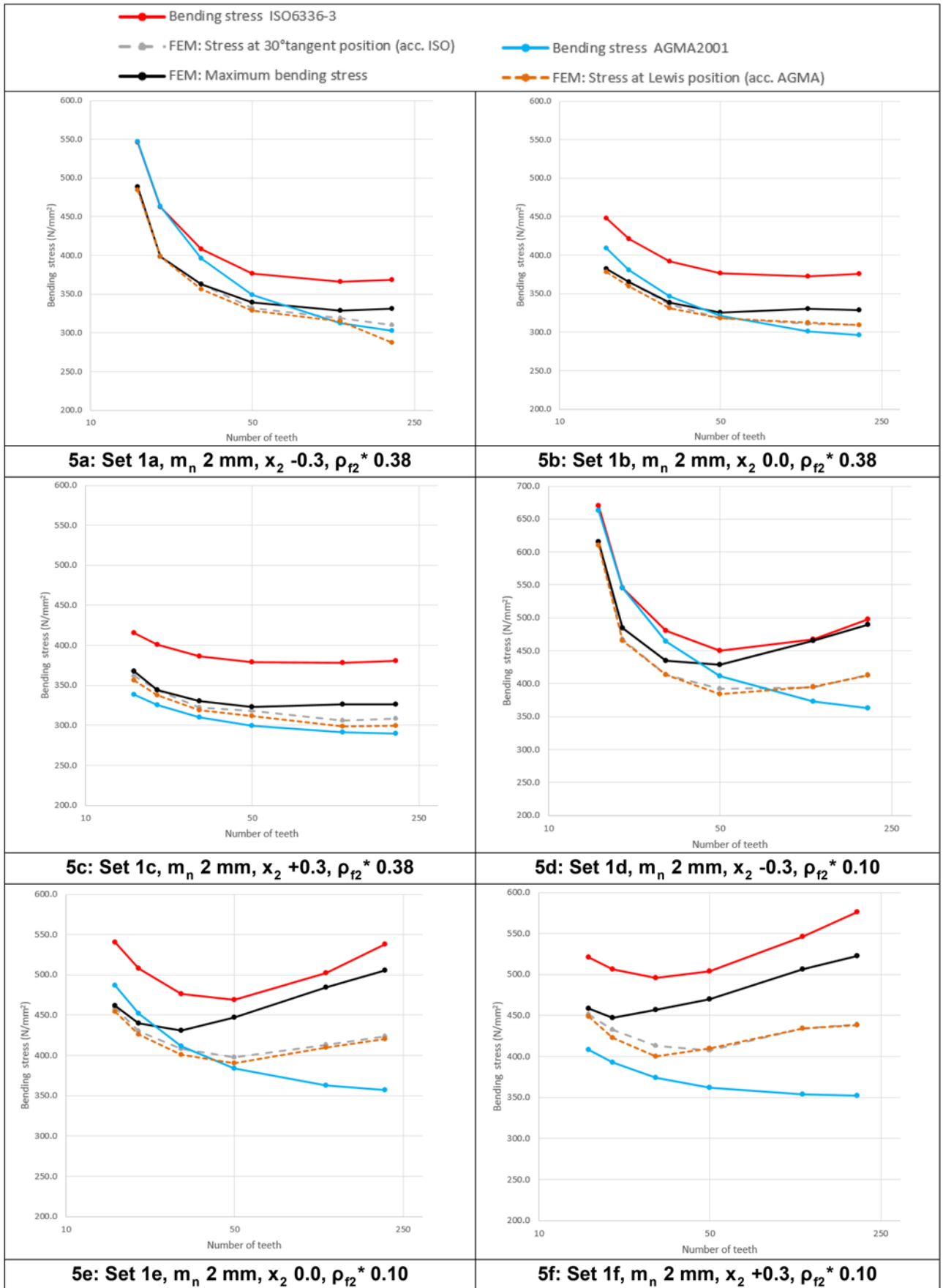


Figure 5 Bending stress σ_{f0} results with module 2 mm gearsets.

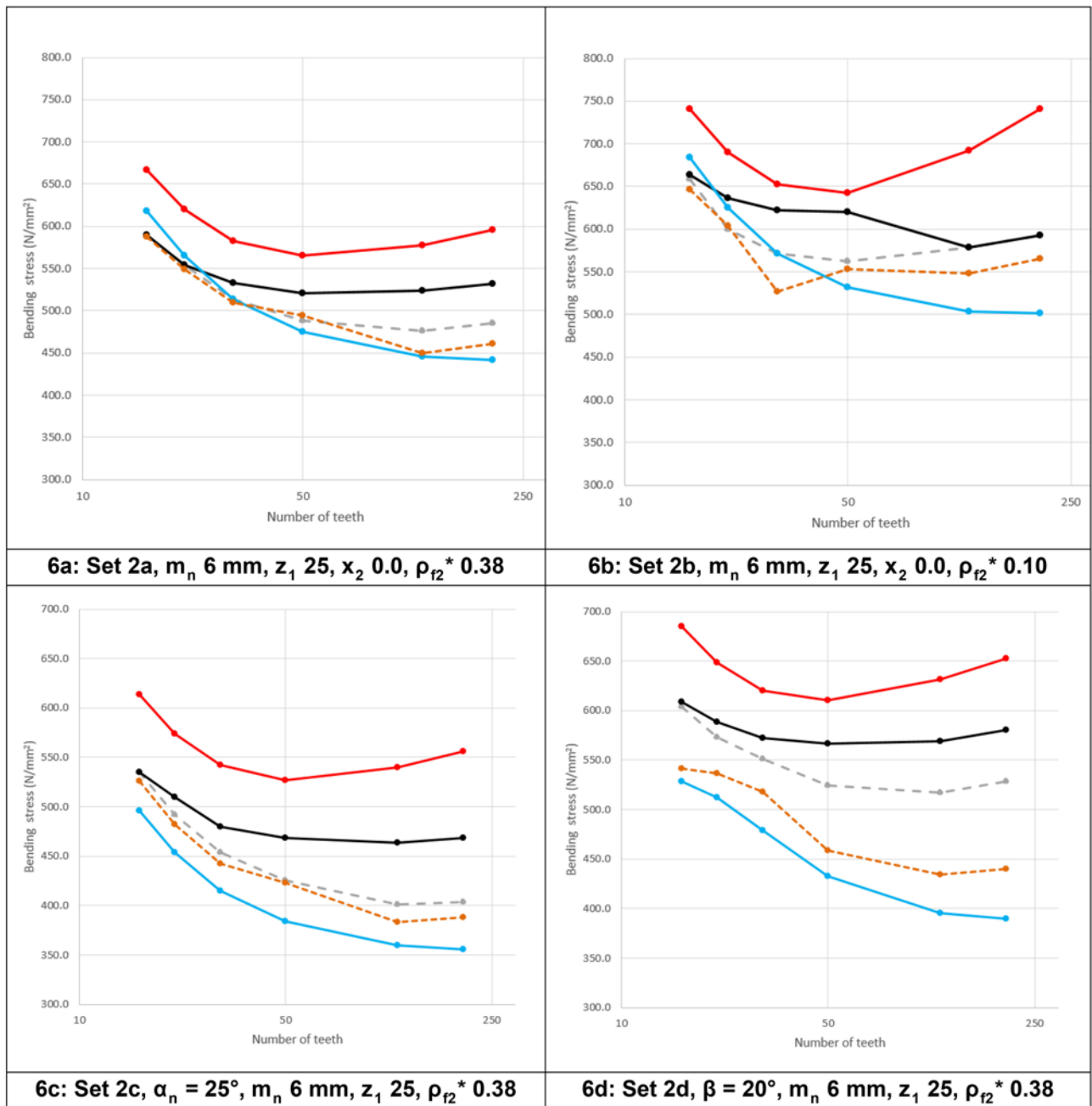


Figure 6 Bending stress results with module 6 mm gearsets.

and Figure 6a–6b are interesting. For example, the curve shapes over the gear tooth number for the maximum FEM stress and for the ISO stress are very similar. ISO stresses are always higher than the FEM results — between 5% to 15%, depending on the case. Therefore ISO values are on the safe side, which is reasonable for a simplified analytical method. In some cases the maximum FEM stress and the FEM stress found at the 30° tangent point are identical, which means that the highest stress found by FEM is located exactly at the 30° tangent point.

AGMA stresses compared to FEM results also show a relatively similar curve shape. But often, AGMA stresses are lower than the FEM results. We found AGMA stresses below FEM stresses specifically for:

- Higher profile shift, x
- Smaller root radius of the reference profile ρ_{FP}^*
- Higher tooth number of the gear

AGMA results are probably too optimistic in these cases. And as the FEM stresses found at the Lewis parabola point (according AGMA) in most cases are a bit smaller than the stresses found at

the 30° tangent point (according ISO), it seems that the 30° tangent is a better approach for the location of the section with highest stress. It must be noted that AGMA 908, with ‘tip loading’ instead of ‘load at HPSTC,’ gives much higher stresses; so ‘tip loading’ is on the safe side, but not ‘load at HPSTC.’

It must be noted that we did not directly compare the FEM results with measured data on the tested gears because we know that ISO 6336-3 rules were tested with measurements (Ref. 12). So, we compared with analytical results obtained by ISO rules; this allowed us to

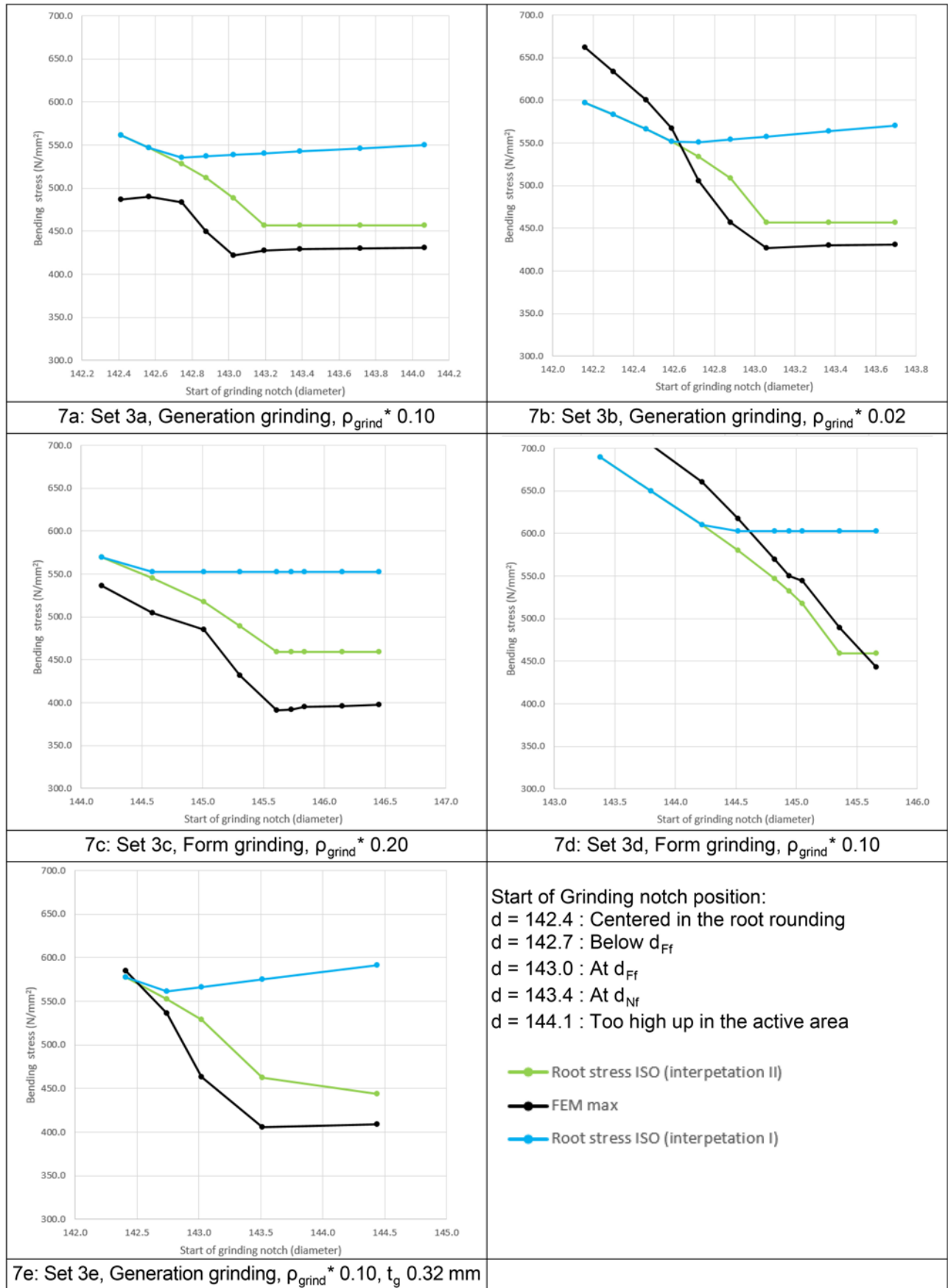


Figure 7 Bending stress results with grinding notch position at different diameters.

check a much higher number of examples. Overall, the tests confirmed that the FEM method is well-adapted to check and compare with stresses according ISO. Therefore, this method can be used for the grinding notch analysis.

Root Stress Calculation by 3-D Finite Element Method

It is very interesting to compare the results from the root stress calculation using a 3-D FEM approach with the results from the bending stresses calculation using the ISO and AGMA standards for helical gears.

But the grinding notch effect as explained in ISO 6336 is based on the equivalent spur gear, so 2-D FEM is best-fitted for this research. In this study the 3-D FEM results will not be used; they will be given in further publications.

Grinding Notch Effect Calculation by 2-D Finite Element Method

The application of the 2-D/FEM calculation, as previously discussed, provides good results and therefore will be used to investigate the grinding notch effect, as grinding notches, especially when form grinding is used, can be quite sharp. Therefore, all calculations were made with very high grid density.

To check the grinding notch effect, we calculated the same gearset (Table 2) with different grinding tool tip height (h_{grind}). So, the position of the grinding notch is

Table 2 Basic gearsets data											
	Module	z_1	x_1	z_2	x_2	h_{grind}^*	P_{grind}^*	Grinding	α_n	β	t_g
Set 3a	6 mm	25	0.25	76	-0.25	varied	0.10	generation	20°	0°	0.16 mm
Set 3b	6 mm	25	0.25	76	-0.25	varied	0.02	generation	20°	0°	0.16 mm
Set 3c	6 mm	25	0.50	76	-0.50	varied	0.20	form	20°	0°	0.16 mm
Set 3d	6 mm	25	0.50	76	-0.50	varied	0.10	form	20°	0°	0.16 mm
Set 3e	6 mm	25	0.25	76	-0.25	varied	0.10	generation	20°	0°	0.32 mm

Note: $b=44$ mm, $T_1=3600$ Nm, Bending safety S_{F2} acc. ISO ca. 1.4
 Grinding Allowance 0.16 mm; pre-manufacturing $h_{ap}^*=1.32$, $\rho_{ip}=0.38$ (Ref. profile final tooth $h_{ip}^*=1.25$)
 FEM: Very high mesh density, clamped at the sides of the segment

varied, starting from a position near the root diameter (in the center of the root rounding), going higher up to the normally used positions (near the active root diameter), to a last point in the active flank range (which, in practice, should be avoided) (Fig. 8).

Generation grinding with two different grinding tip radii and form grinding with two different grinding tip radii is checked, including different grinding allowances (Table 2).

Different gearsets were analyzed, and an extract of the results is displayed (Fig. 7); the most important parameters to check are:

- The height of the grinding tool, h_{grind}
- The tip radius of the grinding tool, ρ_{grind}
- The grinding allowance, q

The radius of the grinding tool is producing the grinding notch radius ρ_g , which will be very different if generating grinding or form grinding is used. A grinding tool radius $\rho_{grind}=0$ will still produce a notch radius of (approximately) $\rho_g=0.17 \cdot m_n$ in a generating grinding

process, but will produce a sharp edge when form grinding is used. The latter is bad practice and should be avoided. We checked generating grinding with tip radius on the tool $\rho_{grind}^*=0.1$ and 0.02; form grinding with $\rho_{grind}^*=0.2$ and 0.1.

The grinding allowance q used in most cases of the study is a standard value according DIN 3972 III, which is often applied in gear manufacturing. If the grinding is increased, then the notch radius ρ_g is unchanged, but the notch depth t_g is bigger, therefore increasing the notch effect. As displayed in Figure 7a and 7e, the stresses are higher in 7e with twice the grinding allowance q .

All the diagrams in Figure 7 show the maximum bending stress σ_{F0} in the root area, calculated with FEM and with the analytical method according ISO6336-3 for Interpretation I and Interpretation II, as discussed earlier. The FEM stresses in all gearsets are highest when the grinding notch is in the lowest position in the center of the root rounding (Fig. 8, right). The higher up the position of the notch,

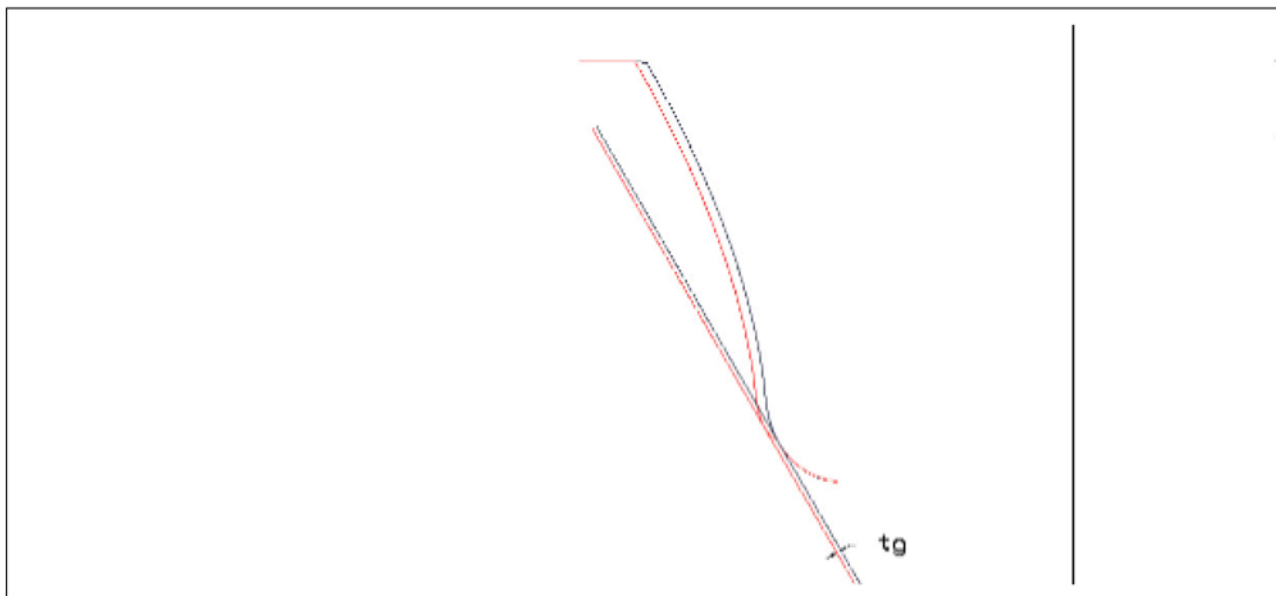


Figure 8 Grinding notch depth t_g according to Interpretation II for a notch position in the d_{Nt} area (left) and for a notch position very low in the root rounding area (right).

the lower are the stresses. From a certain position on, the stresses are constant. Constant stress behavior indicates that the location of the maximum stress is no longer in the grinding notch—but in the root rounding area.

The analytical calculated stresses according ISO, using Interpretation I (constant t_g), demonstrate a very different behavior. The highest value is at the same position as the FEM stress, but with higher position of the notch, the stress first decreases a bit, but then remains constant and even starts to increase slightly (due to the fact that the grinding notch produced by generating grinding is decreasing with higher position of the tool).

The stresses according to ISO, using Interpretation II (t_g used, as indicated in Figure 8, left) is identical to the stress according to Interpretation I in the lowest notch position, but then it decreases significantly to become constant at a higher notch position—or very similar to the FEM results. We found similar behavior between FEM and Interpretation II in all gearsets we checked.

Also important to note is that, with few exceptions, the FEM stress is always lower than the Interpretation II stress, meaning that the ISO approach is on the safe side; the exceptions found are all cases where the notch is in a low position. As already mentioned, gears are

normally not ground so deeply into the tooth rounding area.

The conclusion is that the use of Equation 1 for Y_{sg} according to Interpretation II, yields realistic results; whereas, Interpretation I is greatly overestimating the notch effect when the notch is in a position just beyond the active flank area (the most-often-used procedure in manufacturing).

Conclusion

Depending on the pre-manufacturing process, often a so-called 'grinding notch' is created during grinding at the position where the grinding tool retracts from the flank. The maximum bending stress, which is normally in the tooth root rounding area, is increased due to a grinding notch. ISO 6336-3 disposes a method that considers the grinding notch effect. The application of this method is analyzed in this paper.

The investigation is made with an FEM tool, which is directly and automatically combined with a verification according to ISO 6336. Therefore, many different gearsets could be analyzed, comparing the maximum stress obtained in the FEM analysis with the stress calculated according ISO 6336. To validate the method, first a set of gears without a grinding notch were calculated; FEM, ISO 6336, and AGMA 2101 results are compared. The outcome is very satisfactory in that

good agreement between FEM and ISO results was obtained. It is therefore evident that the method can also be used for the investigation of the grinding notch effect.

The grinding notch depth t_g used in the grinding notch formula in ISO 6336 can be interpreted in two ways. Interpretation I basically does not consider the position of the notch (in the tooth height direction), whereas Interpretation II considers the effective notch depth in dependency of the notch position. Many gearsets with different position of the grinding notch (generated by a different tip height of the grinding tool), different grinding tool tip radius, form and generating grinding processes, and different grinding allowance are analyzed. The FEM results confirmed that the stress increase through a grinding notch significantly depends on the notch position. The results according Interpretation II show good consistency with the FEM results. In contrast, Interpretation I results are overly conservative, partially showing even contradictory (unrealistic) stress values.

As the method to calculate the grinding notch depth t_g and the grinding notch radius ρ_g is not documented in ISO 6336-3, the formulas to obtain these values are explained. ⚙️

Annex A: Formulas Used to Calculate the Grinding Notch Factor Y_{sg}

In ISO 6336-3, only the equation for Y_{sg} is documented, but there is no indication of how to get the notch depth t_g and radius ρ_g . For an outer gear, the notch geometry data can be obtained as follows: All symbols are according to the definitions in ISO 6336-3 (Ref. 4).

All data needed for the form factor Y_F (see previous Root Stress Calculation by 3-D Finite Element Method) (Ref. 4)) must be calculated twice—first for the pre-machining tool, and then for the grinding process.

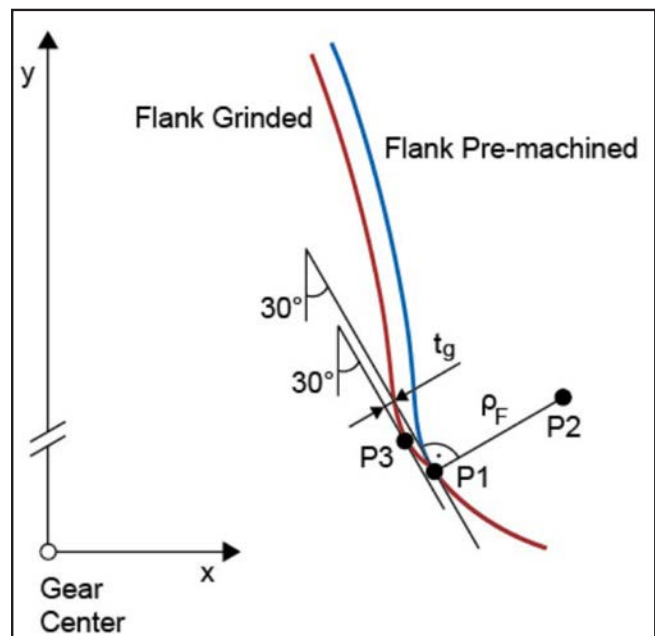


Figure 9 Grinding notch geometry points; P1: 30° tangent point of root rounding; P2: center of root rounding radius; P3: 30° tangent point of grinding notch.

Pre-machining tool data. A first calculation of Y_F with the basic rack profile data of the pre-machined gear — using the pre-machining manufacturing profile shift x_{Epre} — must be made to get s_{nF} , z_n , θ , G , ρ_{fpv} , ρ_{Fv} according to ISO 6336-3.

Point P1 (x_1, y_1): $x_1 = S_{nF}/2$

$$y_{sFn}' = \frac{m_n}{2} \left[z_n \cos\left(\frac{\pi}{3} - \theta\right) + \left(\frac{G}{\cos\theta} - \frac{\rho_{fpv}}{m_n}\right) \right]$$

$$y_1 = y_{sFn}' + \frac{d}{2} \left(1 - \frac{1}{(\cos\beta_b)^2} \right)$$

Point P2 (x_2, y_2): $x_2 = x_1 + \rho_F \cdot \cos\left(\frac{\pi}{3}\right)$

$$y_2 = y_1 + \rho_F \cdot \sin\left(\frac{\pi}{3}\right)$$

Grinding tool data (generation grinding). For a generating grinding process, a second calculation of Y_F with the basic rack profile corresponding to the grinding tool data (Fig. 10) — using the final manufacturing profile shift x_E , h_{grind} for h_{fp} and ρ_{grind} for ρ_{fp} — must be made to get s_n , F_g , θ_g , G_g , ρ_{fpvg} , ρ_{Fg} according to ISO 6336-3.

Point P3 (x_3, y_3): $x_3 = S_{nFg}/2$

$$y_{sFng}' = \frac{m_n}{2} \left[z_n \cos\left(\frac{\pi}{3} - \theta_g\right) + \left(\frac{G_g}{\cos\theta_g} - \frac{\rho_{fpvg}}{m_n}\right) \right]$$

$$y_3 = y_{sFng}' + \frac{d}{2} \left(1 - \frac{1}{(\cos\beta_b)^2} \right)$$

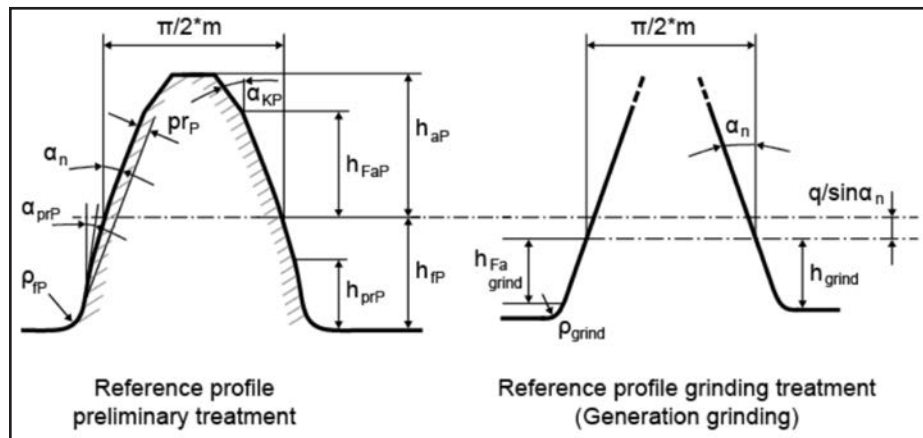


Figure 10 Definition of the gear reference profile for the grinding process.

Grinding notch data.

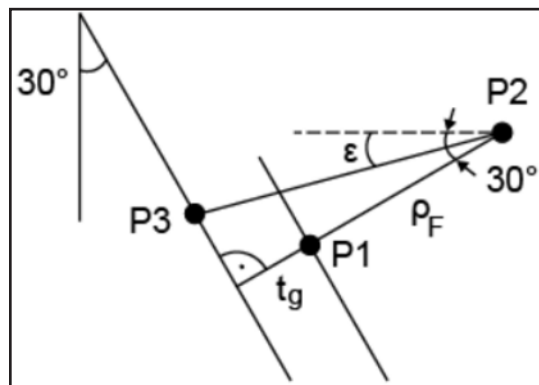


Figure 11 Grinding notch depth t_g .

With $\epsilon = \arctan\left(\frac{y_2 - y_3}{x_2 - x_3}\right)$

we get angle $P1-P2-P3$ $\gamma = \frac{\pi}{6} - \epsilon$

$$\overline{P_2P_3} = \sqrt{(x_2 - x_3)^2 + (y_2 - y_3)^2}$$

Then the grinding notch geometry is obtained with:

$$t_g = \overline{P_2P_3} \cdot \cos(\gamma) - \rho_F \text{ and } \rho_g = \rho_{Fg}$$

In this paper, the formulas for outer gears using generating grinding are documented. The method to get the grinding geometry for form grinding is similar, but simpler, because the notch radius is equal to the grinding tool tip radius. For inner gears, both for generating and form grinding, a very similar approach can be used.

References

1. Wirth, X. "On the Impact of Grinding Notches in Surface Hardened Gears," Doctoral Thesis, 1977.
2. AGMA 2015-1-A01. *Accuracy Classification System — Tangential Measurements for Cylindrical Gears*, AGMA.
3. DIN 3990-3. *Load Capacity of Cylindrical Gears — Part 3*, 1987.
4. ISO 6336-3. *Calculation of Load Capacity of Spur and Helical Gears — Part 3: Calculation of Bending Strength*, 2007.
5. Puchner, O. and A. Kamensky. "Stress Concentration and Notch Effect of Notches Included in a Bigger Notch Area," *Konstruktion* 24 (1972) 127-134.
6. *STplus Cylindrical Gear Calculation software* (developed by FZG Munich).
7. *KISSsoft Calculation Programs*, www.KISSsoft.com.
8. AGMA 908-B89. *Geometry Factors for Determining the Pitting Resistance and Bending Strength of*
9. *Spur, Helical and Herringbone Gear Teeth*, AGMA, 1989.
10. www.code-aster.org.
11. www.salome-platform.org.
12. Wright, A. "A Comparison of the Tooth-Root Stress and Contact Stress of an Involute Spur Gear Mesh as Calculated by FEM and AGMA Standards," Masters Thesis, Rensselaer Polytechnic Institute, June 2013.
13. Hirt, M. "Influence of the Gear Tooth Smoothing on the Stress and Resistance of Spur Gears," Doctoral
14. Thesis, TU München, 1974.
15. ISO 21771. *Gears — Cylindrical Involute Gears and Gear Pairs — Concept and Geometry*, 2007.

Dr. Ulrich Kissling

studied machine engineering (1976-1980) at the Swiss Technical University (ETH), where he also completed his doctoral thesis — "Pneumatic Weft Insertion on Weaving Machines." In 1981 he started his professional career as calculation engineer for a gearbox manufacturing company in Zurich, progressing there to technical manager and ultimately managing director.



Dr. Eng. Ioannis Zotos

has since 2013 been a developer at KISSsoft AG. He previously worked as an R&D consultant in various companies, in fields ranging from aeronautics to automotive and high-precision machines. Zotos holds a Ph.D. in precision maintenance and troubleshooting, an MSc in design of rotating machines, and an MEng in mechanical engineering.



For Related Articles Search

grinding

at www.geartechology.com

For more information.

Questions or comments regarding this paper? Please contact Dr. Ulrich Kissling; ulrich.kissling@kisssoft.ch.